Magneto-mechanical mixing and manipulation of picoliter volumes in vesicles†

Thomas Franke,*[ab] Lothar Schmid,[a] David A. Weitz[b] and Achim Wixforth[a]

DOI: 10.1039/b906569p

Superparamagnetic beads in giant unilamellar vesicles are used to facilitate magnetic manipulation, positioning, agitation and mixing of ultrasmall liquid volumes. Vesicles act as leakproof picoliter reaction vessels in an aqueous bulk solution and can be deliberately conveyed by an external magnetic field to a designated position. Upon application of an external magnetic field the beads align to form extended chains. In a rotating magnetic field chains break up into smaller fragments caused by the interplay of viscous friction and magnetic attraction. This process obeys a simple relationship and can be exploited to enhance mixing of the vesicle content and the outer solution or adjacent vesicle volumes exactly at the position of release.

I. Introduction

Vesicles provide ideal containers for drug delivery or reaction vessels as they consist of a biocompatible soft lipid membrane enclosing a tiny fluid volume. They form an aqueous compartment within a surrounding aqueous bulk solution. Therefore, for applications for a miniaturized laboratory, vesicles offer the opportunity to use the bulk solution continuous-phase also as a component of the reactant rather than as suspending medium, in contrast to containers formed by immiscible water/oil or oil/water emulsions.

In order to manipulate these objects, magnetic or (di)electrophoretic forces[1] can be invoked. The force exerted on a bead by an external magnetic field and its motion in a complex viscoelastic fluid environment provides an interesting physical problem in itself.[2] Such magnetic particles might serve as a versatile tool to locally probe the microrheology of complex fluids[3–5] such as the intracellular non-Newtonian fluid of cells.[6] In addition, superparamagnetic beads align according to the field and form extended chains.[7] A magnetic field gradient generates a force on these magnetic dipole chains whereas a rotational field can be employed to actuate spinning of the chains.

Recently an integrated hybrid platform was introduced to manipulate magnetic particles down to micrometer precision.[8] These Lab-on-a-chip devices combine microfluidics and CMOS technology and can be used for biological applications such as the separation of living cells in microfluidic channels[9] or controlling their motion.[10] On a larger length scale, another group has magnetically actuated drops of water on superhydrophobic surfaces.[11]

The use of magnetic colloids surrounded by a lipid membrane has proven to be a versatile tool in several biomedical applications such as MRI,[12,13] drug delivery[14] and cancer treatment.[15] In such magnetoliposomes the lipid membrane can be directly attached to the magnetic iron core or form a vesicle of several hundred nm size (100 nm–500 nm).[16] These large unilamellar vesicles (LUV) are typically prepared by extrusion and enclose magnetic colloids of nanometer-size (1–10 nm). Giant unilamellar vesicles (GUV) are reported to be formed by a spontaneous swelling process and to enclose magnetic nanoparticles or a ferrofluid.[17,18]

Here, we demonstrate the inclusion of micrometer-sized superparamagnetic beads into the volume of giant lipid vesicles with volumes of order picoliters. These microbeads align to form chains in an external magnetic field. In a rotating magnetic field the chains eventually break up into smaller fragments with chain length depending on the frequency of rotation, viscosity and magnetization. We illustrate the precise control of motion of the vesicles and their utility as stable leakproof containers. Furthermore, we deliberately release the content of the vesicle to induce a chemical reaction and demonstrate that the magnetic beads within the vesicle can even be used as a microstirrer. This enables us to mix the vesicle with the outer bulk solution at exactly the position where its content is released.

II. Manipulation

The preparation of vesicles was done with an electroformation method.[19–21] Briefly, a small amount of lipid in chloroform (10 microliters of an 1 mg/ml solution) was deposited onto two indium tin oxide (ITO) coated glass slides and the organic solvent was evaporated in vacuum for 3 hours. An aqueous solution including the superparamagnetic beads was subsequently added to the same spot of the dried lipid, preswelling the lipid multilayer; this prehydration step enhances the formation of vesicles.[22] Here, it also assures incorporation of the beads into the vesicles. Then, the two ITO plates were mounted in parallel and an

[a]*University of Augsburg, Experimental Physics 1, Microfluidics Group, Universitätsstr. 1, D-86159 Augsburg, Germany. E-mail: thomas.franke@physik.uni-augsburg.de; lothar.schmid@physik.uni-augsburg.de*
[b]*School of Engineering and Applied Sciences, Harvard University, Cambridge, MA, 02138, USA*

† Electronic supplementary information (ESI) available: Movies: aggregation_a.mov, motion1_a.mov, motion2_a.mov and mixing_permeation_a.mov. These movies can be played with Apple QuickTime which can be obtained from http://www.apple.com/quicktime/download/. See DOI: 10.1039/b906569p

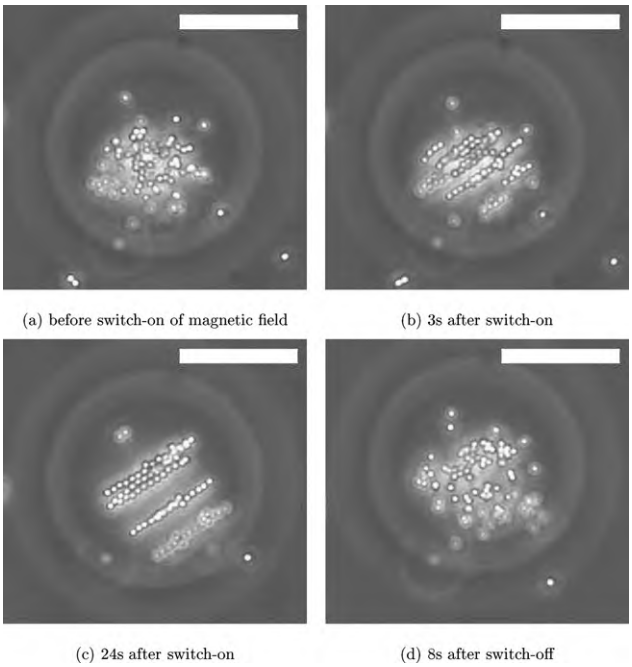

Fig. 1 Magnetic field induced aggregation of superparamagnetic beads in a vesicle. The scale bar represents 20 μm. (a) Without magnetic field, the beads diffuse freely within the vesicle volume. (b) 3 seconds after an external magnetic field $B \approx 2.3$ mT is applied, the beads successively aggregate to form extended chains. (c) After 24 seconds all beads have aligned into several long chains. (d) 8 seconds after switching off the field the beads have dispersed again. The formation and decomposition of chains is reversible and was induced several times. See movie aggregation_a.mov in the ESI.†

electric field of 1 V/mm at a frequency of 10 Hz was applied for at least 3 hours. Usually, just before harvesting the vesicles, the voltage was increased to 10 V at 1 Hz to facilitate the separation of vesicles. Using this method, many giant unilamellar vesicles, with diameters larger than 10 microns, were successfully formed, containing dozens of superparamagnetic beads.

The superparamagnetic beads within the vesicles assemble into a line to form a chain upon application of an external magnetic field (see Fig. 1). The minimum magnetic field strength $B_{\min}$ required to manipulate a single superparamagnetic bead can be estimated from its magnetic susceptibility, $\chi = 1.4$. The magnetic moment of a spherical paramagnetic particle of volume V is given by $m = V\chi B/\mu_0$ and its potential energy is $E_{pot} = -mB = -\chi VB^2/\mu_0$, with μ_0 denoting the magnetic constant. Therefore, to exceed thermal energy, a field of $B_{\min} \approx 59$ μT is necessary for a 1-μm-diameter bead. Because this field is so low, it can easily be obtained using a permanent magnet or even generated by a current flowing through a microwire.[8]

The magnetic force acting on the bead is proportional to the gradient of the field and the susceptibility difference $\Delta\chi$ between water and bead.

$$F = \frac{V\Delta\chi}{\mu_0}(\vec{B}\cdot\nabla)\vec{B} \qquad (1)$$

Although this formula is widely used, recent results suggest that it should be expanded with an additional term reflecting an initial

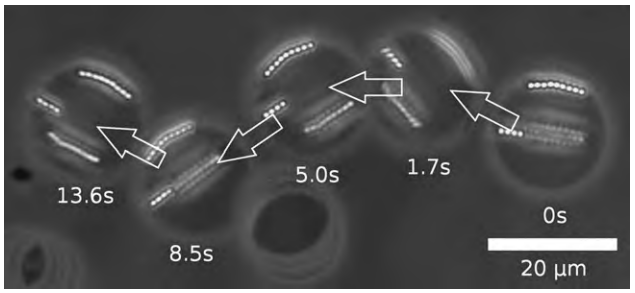

Fig. 2 Micrograph of a vesicle which includes about 20 superparamagnetic beads being chained up. We control the magnetic field gradient to direct the vesicle along a designated path. The mean velocity of the vesicles is $v = 7$ μm/s. The image is an superposition of snapshots of the vesicle at different times as indicated. The arrows indicate direction of motion. See movies motion1_a.mov and motion2_a.mov in the ESI.†

magnetization.[2] It can be used to estimate the parameters needed to actuate a vesicle in solution. The magnetic force must balance the hydrodynamic drag force, approximated by Stokes' law $F_d = 6\pi\eta rv$, where v is the velocity of the vesicle of radius r and η the viscosity of the surrounding fluid. To move a vesicle with $r = 20$ μm containing 30 superparamagnetic beads with a diameter of 1 μm and a magnetic susceptibility $\chi = 1.4$ at a speed of 1 μm/sec in water, a field gradient of $B_x\partial B_x/\partial x = 0.22$ T^2/m is necessary.

The direction of motion of a vesicle can be controlled by the direction of the magnetic field gradient allowing it to be maneuvered to any designated position; an example of the motion of a vesicle driven by a magnetic field is shown in Fig. 2.

In addition, application of a rotating magnetic field causes the superparamagnetic chain to rotate inside the vesicle, eventually causing a rotation of the vesicle itself. In this way, the chain acts as a microstirrer in a closed volume and can be used to enhance mixing.

To confirm the integrity of the lipid membrane and to prove that the vesicle is not leaking any content, we added fluorescein at a 100 mM concentration to the continuous phase fluid. At such high concentrations, fluorescein is self-quenching, making it very sensitive to even small permeation of water through the lipid membrane. Any exchange of liquid across the membrane would therefore reduce the self-quenching and consequently increase the fluorescence. We estimate the detection limit for leaking to be 1/1000 of the respective vesicle volume as determined by a calibration of intensity against fluorescein concentration. We encapsulated magnetic beads and aligned them into chains with an external magnetic field. As a vesicle is moved across the microchamber, repeated rotations of the chains were initiated without detection of any fluorescent signal. This demonstrates that the vesicle is leakproof. However, subsequent addition of the membrane-porating surfactant Triton-X causes permeation of water through the membrane and a strong increase in fluorescent signal as demonstrated in Fig. 3. This also shows that we can deliberately induce a reaction of the vesicle's content with the bulk at a designated position.

III. Mixing

Generally, after releasing the content of the vesicle, the intravesicular fluid volume mixes diffusively with the surrounding

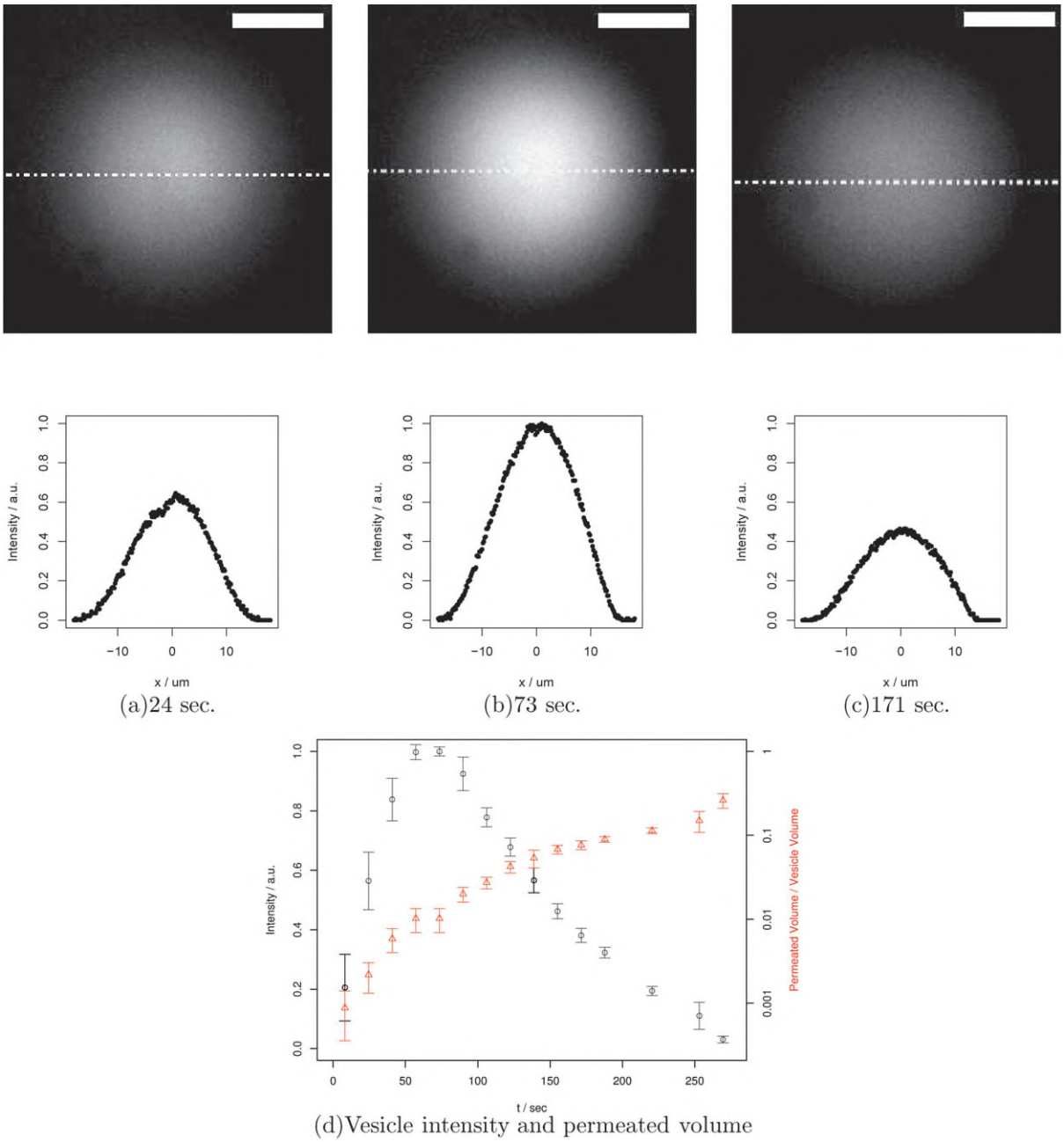

Fig. 3 A vesicle with magnetic beads was positioned and subsequently the membrane was dissolved. (a) Initial increase of fluorescent signal at $t = 24$ sec; (b) Maximum of fluorescence is reached at $t = 73$ sec; (c) Decreasing intensity at $t = 171$ sec; The white scale bars represent 10 μm; The plots below correspond to the respective micrographs above and show the fluorescence intensity profile along the white dash-dotted line; (d) The integrated intensity of the entire vesicle (black circles) and the permeated volume relative to the volume of the vesicle (red triangles) as determined by a calibration of intensity against concentration. See also movie mixing_permeation_a.mov in the ESI.†

bulk solution. Here, we show that the magnetic beads within a vesicle can be also used to enhance mixing by active agitation. We apply a rotating external magnetic field to a number of magnetic chains.

The chain length of agglomerated beads depends critically on the frequency of chain rotation,[23,24] which is a fundamental parameter for mixing efficiency.[25] The bead chains split into smaller fragments when the frequency is increased above a critical frequency $\omega_{cr.}$, whose value depends on the number of beads n and the viscosity of the bulk solution η.

We propose a simple model: Opposing forces act upon the two sides of the rotating chain due to hydrodynamic drag (see model Fig. 4). The drag force F_i acting on bead i can be estimated by Stokes' law[26,27]

$$F_i = 6\pi r\eta v_i = 3\pi d^2\eta\omega \cdot i \qquad (2)$$

where r, d is the radius and diameter of the beads, η is the viscosity of the fluid, v_i the velocity of the respective bead, and ω denotes the angular velocity of the rotating chain (which is the

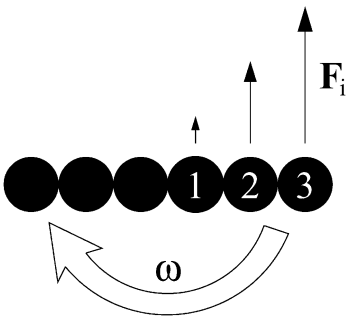

Fig. 4 Sketch of a chain composed of superparamagnetic beads. A hydrodynamic drag force F_i acts on bead i (numbering as indicated in the figure) as a result of the rotation of the chain as a whole. The aggregate is assumed to stick together by next neighbor interaction.

same as the angular velocity of the rotating field). The overall drag force F_D acting on one half of the microstirrer therefore is given by the sum of all forces F_i acting on the beads forming this half of the chain:

$$F_D = \sum_{i=1}^{n/2} F_i = \frac{3}{8}\pi d^2 \eta \omega n^2 = \frac{3}{4}\pi^2 d^2 \eta f n^2 \tag{3}$$

Here we replaced the angular velocity ω of the field with its frequency $f = \omega/2\pi$. This formula applies only if the bead number n is even; for an odd number of beads in the chain, the index i runs to $(n - 1)/2$, and n^2 must be replaced by $n^2 - 1$. However, for all relevant cases this is negligible as already for 7 beads the deviation is only 2%. This tangential drag force must be balanced by the attractive magnetic force acting between the beads that make up the chain. The direction of the attractive force is approximately parallel to the line connecting two adjacent beads. Eventually, close to the critical angular velocity, the chain adopts an S-shape.[28] Therefore, the relevant length of the chain in Eq. 3 is reduced; however, observations suggest that this is a minor effect.[29]

To estimate the attractive force between adjacent beads, we assume that a bead with magnetic moment m interacts only with its next neighbor and thus exhibits a potential energy of

$$U = \frac{m^2}{2\pi\mu_0}\frac{1}{l^3} = \frac{\mu_0}{2\pi}V^2M^2\frac{1}{l^3} \tag{4}$$

Here, M is the magnetization and V the volume of the bead, l denotes the distance of adjacent beads. In a magnetic field $B \approx 15$ mT a bead of diameter $d = 1$ μm gains a magnetic moment $m = 8.8 \times 10^{-15}$ A m². Here, we have taken the magnetic susceptibility to be $\chi = 1.4$ (as reported by the supplier Invitrogen) and estimated the strength of the field at a distance of 8.5 mm between the bead and the center of the permanent magnet. Hence the attractive force, which is an estimate for the critical drag force strength of chain breakup, is

$$F_M = -\left.\frac{\partial U}{\partial l}\right|_{l=d} \approx 46\ \text{pN} \tag{5}$$

At the point of chain breakup, the attractive magnetic force F_M balances the drag forces F_D. Therefore, the number of beads n can be calculated from equations 3 and 5 to be

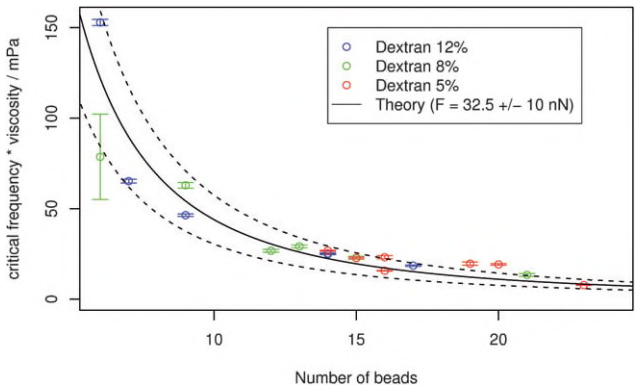

Fig. 5 Demonstration of the critical frequency of chain breakup depending on the length of the chain (number of superparamagnetic beads). Experiments were done in several dextrane solutions of different viscosities and are displayed in red, blue and green respectively. Plotted is the shear strength against number of beads (masterplot). The solid line is a $1/n^2$ fit according to our model Eq. 6 and shows reasonable agreement. The dashed lines show the error range.

$$\frac{1}{n^2} = 9\frac{\eta\omega}{\mu_0 M^2} \tag{6}$$

This result is proportional to the Mason number $Ma = 12^2\eta\omega/\mu_0 M^2$.[23–25,27] The Mason number in our experiments varies between $0.006 < Ma < 0.022$ in water. To test our model, we plot the results of our experiments for chain breakup at different viscosities together with the theoretical model in Fig. 5. The masterplot exhibits a quadratic dependence of the critical shear stress on the number of beads, consistent with the predictions of Eq. 3, for all viscosities measured. In addition, exploiting Eq. 3 we can extract the critical force from the $1/n^2$ fit to be 32.5 pN, in good agreement with our estimate (Eq. 5). Here we employ that $F_M = F_D$ at the critical frequency. Thus, our model correctly accounts for the basic physics of this behavior.

To quantify the fluid flow, we used small tracer particles in close proximity to the microstirrer. The overall trajectories of these tracers are circles around the center of the microstirrer with additional small oscillations as shown in Fig. 6.[30,31] These oscillations have the same frequency as the magnetic stirrer. The angular velocity of the overall circular motion of individual tracer beads decreases with distance from the center of the stirrer as shown in the inset of Fig. 6. Therefore, the spatial period length of the oscillating trajectories decreases.

The efficiency of mixing depends on the diffusion coefficient of the particles that are to be mixed. With small particles, mixing is dominated by diffusion, while for large particles, advection is more important. The ratio of these two effects is characterized by the Péclet number $Pe = Lv/D$, with the characteristic length L, velocity v and diffusion coefficient D. Calhoun *et al.* characterize the mixing efficiency by a mixing rate.[25] They determined the dependence of the mixing rate on the Péclet number and found that for high Péclet numbers $Pe \gtrsim 50$, mixing is dominated by stirrer-induced advection and diffusion effects are negligible.[25] For typical chain dimensions $L \approx 10$ μm and stirrer frequencies $f = 3$ Hz of our mixer we estimate the diffusion coefficient for

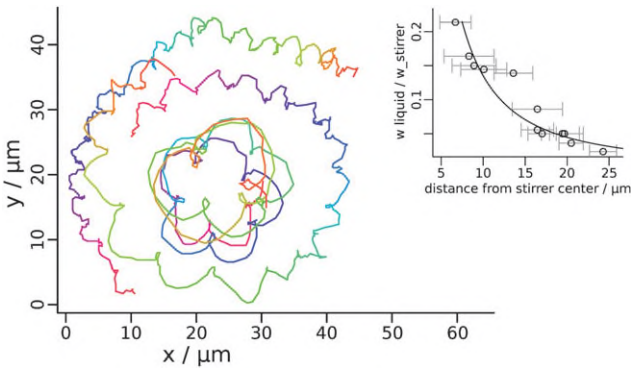

Fig. 6 Typical trajectories of latex tracer beads as obtained from particle tracking. Coloring was used to distinguish overlappping trajectories of particles. The inset shows the angular velocity of the tracer particles normalized by stirrer angular velocity depending on distance r from the center of the stirrer. Open circles are the experimental data as obtained from tracking individual tracer beads. The solid line is a fit with r_0^2/r^2. The best fit of the experimental data is for $r_0 = 3.94$ µm. The r_0^2/r^2-dependence is expected for 2-dimensional cylindrical Couette flow around a rotating cylinder of radius r_0.[33]

which our system is in the transitional regime at $Pe = 50$ above which mixing is effective.

$$D = 9.4 \times 10^{-12}\ \mathrm{m^2/s} \tag{7}$$

Employing the Stokes-Einstein relation $D = kT/6\pi\eta r$, this diffusion coefficient corresponds to a radius $r = 23$ nm of a particle in water. Hence, the proposed mixing mechanism is particularly effective for nanoparticles $\gtrsim 20$ nm. Therefore, various particles used for drug delivery systems such as viral particles or polymer capsules can be mixed efficiently. Moreover the uptake of those particles into a target cell can be improved by increasing the rate of cell-particle collisions by effective mixing. This is highly important, for example to enhance the transfection efficiency of gene transfer experiments of cancer cells.[32]

IV. Conclusion

We have demonstrated that vesicles with enclosed superparamagnetic microbeads have the potential to both position and mix picoliter volumes in microreactors. We describe the breakup of the magnetic chains both experimentally and theoretically. Furthermore, we have shown that stirring with magnetic chains is an effective way to enhance mixing of nanoparticles. Giant unilamellar vesicles with superparamagnetic microbeads thus represent a versatile tool in microfluidic devices. It would be particularly interesting to use these objects on a "lab-on-a-chip" platform where magnetic field control is integrated on the chip.[8]

Acknowledgements

This work was supported by NIM (Nanosystems Initiative Munich), the DFG Priority Program "Nano- and Microfluidics" (SPP 1164) and the Bayerische Forschungsstiftung.

References

1 T. P. Hunt, D. Issadore and R. M. Westervelt, *Lab on a Chip*, 2008, **8**, 81–87.
2 S. S. Shevkoplyas, A. C. Siegel, R. M. Westervelt, M. G. Prentiss and G. M. Whitesides, *Lab on a Chip*, 2007, **7**, 1294–1302.
3 M. Keller, J. Schilling and E. Sackmann, *Review of Scientific Instruments*, 2001, **72**, 3626–3634.
4 F. Ziemann, J. Rädler and E. Sackmann, *Biophysical Journal*, 1994, **66**, 2210–2216.
5 F. Amblard, B. Yurke, A. N. Pargellis and S. Leibler, *Review of Scientific Instruments*, 1996, **67**, 818–827.
6 C. Wilhelm, J. Browaeys, A. Ponton and J.-C. Bacri, *Phys. Rev. E*, 2003, **67**(1), 011504.
7 S. Melle, M. A. Rubio and G. G. Fuller, *Phys. Rev. Lett.*, 2001, **87**(11), 115501.
8 C. S. Lee, H. Lee and R. M. Westervelt, *Applied Physics Letters*, 2001, **79**(20), 3308–3310.
9 N. Xia, T. P. Hunt, B. T. Mayers, E. Alsberg, G. M. Whitesides, R. M. Westervelt and D. E. Ingber, *Biomedical Microdevices*, 2006, **8**(4), 299–308.
10 H. Lee, Y. Liu, D. Hamb and R. M. Westervelt, *Lab on a Chip*, 2007, **7**, 331–337.
11 A. Egatz-Gómez, S. Melle, A. García, S. A. Lindsay, M. Márquez, P. Domínguez-García, M. A. Rubio, S. T. Picraux, J. L. Taraci, T. Clement, D. Yang, M. A. Hayes and D. Gust, *Applied Physics Letters*, 2006, **89**, 034106.
12 M. S. Martina, J. P. Fortin, C. Ménager, O. Clément, G. Barratt, C. Grabielle-Madelmont, F. Gazeau, V. Cabuil and S. Lesieur, *J. Am. Chem. Soc.*, 2005, **127**, 10676–85.
13 C. Rivière, M.-S. Martina, Y. Tomita, C. Wilhelm, A. T. Dinh, C. Ménager, E. Pinard, S. Lesieur, F. Gazeau and J. Seylaz, *Radiology*, 2007, **244**(2), 439–448.
14 C. Sun, J. S. H. Lee and M. Zhang, *Advanced Drug Delivery Reviews*, 2008, **60**(11), 1252–1265.
15 J.-P. Fortin-Ripoche, M. S. Martina, F. Gazeau, C. Ménager, C. Wilhelm, J.-C. Bacri, S. Lesieur and O. Cl m′ent, *Radiology*, 2006, **239**, 415–424.
16 S. J. H. Soenen, M. Hodenius and M. D. Cuyper, *Nanomedicine*, 2009, **4**(2), 177–191.
17 O. Sandre, C. Ménager, J. Prost, V. Cabuil, J.-C. Bacri and A. Cebers, *Phys. Rev. E*, 2000, **62**(3), 3865–3870.
18 G. Beaune, C. Ménager and V. Cabuil, *J. Phys. Chem. B*, 2008, **112**, 7424–7429.
19 M. I. Angelova and D. S. Dimitrov, *Faraday Discuss. Chem. Soc.*, 1986, **81**, 303–311.
20 M. I. Angelova, S. Soléau, P. Meleard, J. F. Faucon and P. Bothorel, *Prog. Colloid Polym. Sci*, 1992, **89**, 127.
21 L.-R. Montes, A. Alonso, F. M. Goñi and L. A. Bagatolli, *Biophys. J.*, 2007, **93**(10), 3548–3554.
22 D. Needham and E. Evans, *Biochemistry*, 1988, **27**, 8261.
23 S. Melle, G. G. Fuller and M. A. Rubio, *Phys. Rev. E*, 2000, **61**(4), 4111–4117.
24 S. Melle, O. Calderon, M. Rubio and G. Fuller, *Journal of Non-Newtonian Fluid Mechanics*, 2002, **102**(14), 135–148.
25 R. Calhoun, A. Yadav, P. Phelan, A. Yuppu, A. Garcia and M. Hayes, *Lab on a Chip*, 2006, **6**, 247–257.
26 A. Yadav, R. Calhoun, P. Phelan, A. Vuppu, A. Garcia and M. Hayes, *IEE Proc.-Nanobiotechnol.*, 2006, **153**(6), 145–150.
27 S. Melle, O. G. Calderòn, M. A. Rubio and G. G. Fuller, *Phys. Rev. E*, 2003, **68**, 041503.
28 A. K. Vuppu, A. A. Garcia and M. A. Hayes, *Langmuir*, 2003, **19**(21), 8646–8653.
29 I. Petousis, E. Homburg, R. Derks and A. Dietzel, *Lab on a Chip*, 2007, **7**, 1746–1751.
30 A. K. Vuppu, A. A. Garcia, S. K. Saha, P. E. Phelan, R. Calhoun and M. A. Hayes, in *Richard Tapia Celebration of Diversity in Computing Conference*, pp. 1–8, 2003.
31 A. K. Vuppu, A. A. Garcia, M. A. Hayes, K. Booksh, P. E. Phelan, R. Calhoun and S. K. Saha, *Journal of Applied Physics*, 2004, **96**, 6831–6838.
32 R. Bausinger, K. von Gersdorff, K. Braeckmans, M. Ogris, E. Wagner, C. Bräuchle and A. Zumbusch, *Angewandte Chemie*, 2006, **118**(10), 1598–1602.
33 E. Guyon, J.-P. Hulin and L. Petit, *Physical Hydrodynamics*, Oxford University Press, 2000.